

Development and validation of a full model of a four-headed neuroimaging single-photon emission computed tomography scanner

Blair A. Johnston^{a,b}, Alice Nicol^c, Alison Bolster^d and Jamie Wright^{c,d,e}

Objective The Nucline X-Ring 4R is a four-headed gamma camera dedicated to neuroimaging. In this paper, we describe and validate a GATE (Geant4 Application for Tomographic Emission) model of the Nucline X-Ring 4R.

Materials and methods Images produced during model simulations were compared with those acquired experimentally to confirm the model was an accurate representation of the scanner. The most commonly reported measurements used to validate a GATE model include energy resolution, spatial resolution and sensitivity. In addition to the commonly reported static imaging measures, single-photon emission computed tomography (SPECT) spatial resolution was investigated to confirm that the model produces similar SPECT images to the experimental output.

Results The experimental full-width at half-maximum was calculated to be 12.3 keV, which corresponds to an energy resolution of 8.8%. The simulated full-width at half-maximum was measured to be 12 keV, giving an energy resolution of 8.6%. The average spatial resolutions were found to be well matched (5.69 mm – simulated and 5.64 mm – experimental). However, the sensitivity was overestimated using the GATE model (47.8 and 54.3 cps/MBq) compared with the values

obtained experimentally (42.7 and 44.3 cps/MBq). Finally, the simulated SPECT spatial resolution images were found to produce qualitatively comparable results.

Conclusion The model developed has been shown to produce similar results and images to those obtained experimentally. This model has the potential to simulate patient scans with the aim of improving patient care by optimizing scanner protocols. *Nucl Med Commun* 40:14–21 Copyright © 2018 Wolters Kluwer Health, Inc. All rights reserved.

Nuclear Medicine Communications 2019, 40:14–21

Keywords: Geant4 Application for Tomographic Emission model, Nucline X-Ring 4R, single-photon emission computed tomography simulation

^aSchool of Medicine, Dentistry and Nursing, University of Glasgow, ^bMRI Physics, ^cDepartment of Nuclear Medicine, Queen Elizabeth University Hospital, ^dDepartment of Nuclear Medicine, Glasgow Royal Infirmary, NHS GGC, Glasgow, UK and ^eHermes Medical Solutions AB, Stockholm, Sweden

Correspondence to Blair A. Johnston, MRI Physics, Level 2, ICE Building Queen Elizabeth University Hospital Campus, 1345 Govan Road, Glasgow G51 4TF, UK Tel: +44 141 451 6850; fax: +44 141 452 6850; e-mail: Blair.Johnston@glasgow.ac.uk

Received 28 June 2018 Revised 26 September 2018 Accepted 8 October 2018

Introduction

There are many Monte Carlo codes available for nuclear medicine and general-purpose applications including SimSET [1], SIMIND [2], Geant [3], Penelope [4], EGS [5] and MCNP [6]. An increasingly popular Monte Carlo code for modelling imaging systems is GATE (Geant4 Application for Tomographic Emission [7]), which is an abstraction layer built on top of Geant4. GATE is popular because of the user-friendly scripting language, the fact it is well tested, the ability to accurately model unusual geometry and a strong record in the literature for producing results that closely match experimental results. The main disadvantage of GATE simulations is that they tend to take a much longer time than other Monte Carlo packages because of the lack of assumptions made by the code.

One of the most prominent early publications using GATE, by Staelens *et al.* [8], developed and validated a model of a dual-headed Phillips AXIS camera. They reported the relative importance of modelling each component of the

scanner head by assessing the percentage of scattering events that took place in each component. The authors found that at low energies [such as the γ photons emitted by technetium-99m (^{99m}Tc)], developing an accurate model of the back-compartment is less important as the vast majority of scattering events take place within the phantom/patient and collimators [8].

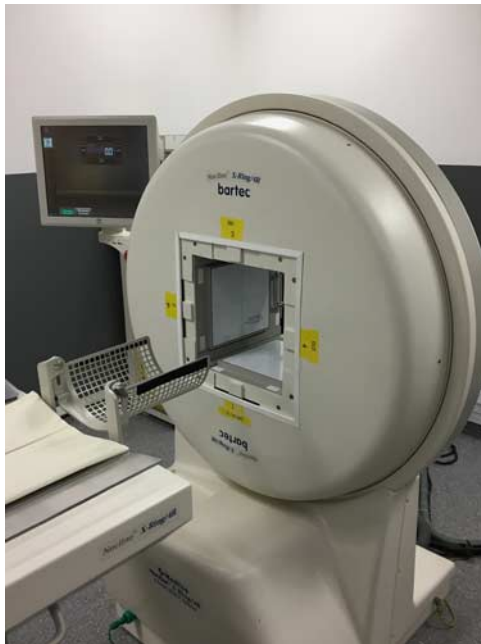
Another early paper using GATE focused on validating the use of indium-111 in a single-photon emission computed tomography (SPECT) simulation of a GE DST-XLi scanner model [9]. The GE DST-XLi was also investigated in high energy radioisotope simulations, alongside the GE Millennium VG scanner (GE) [10]. A more recent study by Momenzhad *et al.* [11] reported the development of a dual-headed Siemens E.Cam gamma camera system using GATE.

A major advantage of GATE is its ability to model unusual scanner geometries and prototype scanners. For example, Imbert *et al.* [12] and Mao *et al.* [13] used GATE to create

and test a heart-centric semiconductor cadmium zinc telluride D-SPECT camera model and a stationary cardiac SPECT system with segmented slant hole collimators respectively. A study by Alzimami and colleagues used GATE to investigate whether replacing NaI(Tl) crystals in SPECT heads with a new crystal material, LaBr₃:Ce (cerium-doped lanthanum crystal), could provide sufficient benefits such that it could be used for both 511 keV ¹⁸F-FDG SPECT and lower-energy SPECT acquisitions [14]. Similarly, Myronakis *et al.* [15] used GATE simulations as part of an attempt to find the optimal pixel size and thickness for a cadmium zinc telluride semiconductor detector operating over the range of low-energy SPECT up to the 511 keV PET energy. Finally, two publications by Vieira *et al.* [16,17] showed a clinical utility using validated GATE models. The first publication by Vieira *et al.* [16], describes the model validation for a GE Millennium MG SPECT gamma camera using GATE. Following this work, Vieira and colleagues then aimed to use the validated model to determine whether differing radio-pharmaceutical activity levels and therefore the number of counts/pixel and total counts per simulation, in a gated-SPECT acquisition would alter the estimates of myocardial function [17].

The Nucline X-Ring 4R scanner (Fig. 1) is a high-resolution, four-headed gamma camera dedicated to brain imaging. The aim of this study was to develop an accurate model of this scanner using GATE and validate it by comparing simulated images with both experimental data and the manufacturer

Fig. 1



The Nucline X-Ring 4R neuroscanner.

specifications. In this study, we aimed to investigate the performance of a four-headed neuroimaging SPECT system that has not been modelled previously and to validate the model using both static and tomographic acquisitions. If a model can be demonstrated to provide an accurate representation of the scanner then it can be used to optimize clinical protocols and reconstruction methods, potentially on a case-by-case basis.

Materials and methods

The GATE model of the Nucline X-Ring 4R scanner (Mediso, Budapest, Hungary) was developed using a combination of information provided by the manufacturer and direct measurements. To reduce the variability when comparing images from both the experimental and simulated systems, the output from the simulated data was converted and imported into the Hermes Medical Solutions software package [18] for reconstruction and analysis, as is performed routinely for the scanner data.

Computing

Root v5.34.36, Geant 4.9.6 and Gate v7.0 were installed on a 6×3.33-GHz processor core Linux PC running Ubuntu 12.04 LTS (Canonical, London, UK). Static imaging simulations were performed using a single processor core but the SPECT imaging simulation divided the simulation between all six cores using the inbuilt cluster computing application programming interface.

An initial aim of the study was to simulate sources with the same radionuclide activity and acquisition times as used to acquire clinical or phantom quality control data routinely. However, it was discovered that more computing power than was available during the project would be required in order to achieve this. The target was therefore revised to simulate sources with a similar level of radionuclide activity but with one-tenth of the acquisition time used routinely.

To perform the SPECT simulations with the revised parameters in a reasonable timeframe, both processor parallelization and the angular response function (ARF) method [19] were required. The ARF method uses the direction and energy of each photon to determine the probability of the photon being detected by the crystal. ARF requires an initial full simulation to generate the information for each collimator design, this information is then stored in ARF tables that can be used to determine the probability of an individual photon being detected given its direction and energy at the collimator surface. Therefore future simulations stop tracking photons at the collimator surface and assign the probability of each photon being detected. The time taken to track photons through the collimators is a particular issue in the high-resolution scanner modelled as the time taken increases with collimator resolution. The use of ARF created a significant speedup factor (~2).

GATE provides an interface for cluster computing software, with the default cluster management code being

Condor [20]. This application splits the simulation into smaller clusters that run in parallel on separate processors and merges the output after each cluster has run. In addition to utilizing cluster computing to reduce simulation time, it also resolved another issue encountered in GATE. When attempting to run simulations with high activity, it was discovered that the simulations would crash on reaching a certain point in the simulation (~4.2 billion simulated events). The reason for this crash was discovered to be due to the fact that the GATE tracks the number of events (photons) that have been simulated using a 32-bit unsigned integer. However, this has a limit of ~4.2 billion ($2^{32} = 4\,294\,967\,296$). Cluster computing helped to work around this ‘maximum events’ issue, by splitting the simulation into clusters of fewer than 4.2 billion events – allowing simulations to be performed using clinical levels of activity that are comparable with the real scanner.

Whilst the time taken to perform GATE simulations is noted as an issue in many publications, for this study it was a particular issue given the limited computing power available and the radionuclide activities simulated. GATE publications [8,21–24] simulating clinical level radionuclide activity acquisitions typically use many more processors; while many of the currently published simulations reported to run on single PCs used much lower activities, such as 300 million emitted photons over the course of a simulation [10]. For comparison, a typical ^{99m}Tc HMPAO brain perfusion scan would contain over 60 000 million emitted photons from the brain alone, assuming a 5.8% brain uptake [25] of 600 MBq administered activity for a 30 min scan. In this study, the largest simulation contained 57 600 emitted particles.

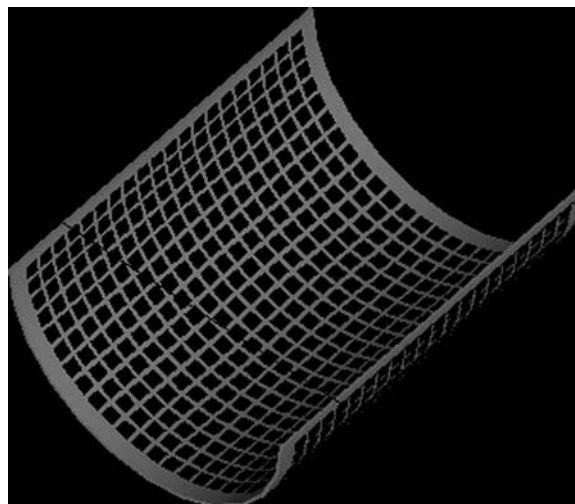
Even using ARF and cluster computing, simulating a 300 MBq source for a total of 32 min was still projected to take more than 50 days to complete. This meant that the longer simulations using high activity levels still would take an unfeasible amount of time to run, given the resources available. The time of each projection was therefore reduced by a factor of 10 to reduce the time taken for each simulation.

Camera model

The Nucline X-Ring 4R scanner contains four detector heads. The model of this scanner included the collimators, the crystal, the back-compartment [an approximation of the photomultiplier tubes (PMTs) and electronics] and all shielding. In addition, a number of different phantoms and supports (such as the headrest shown in Fig. 2) were modelled.

Staelens *et al.* [8] discussed the importance of correctly modelling the collimators and the issues that could arise if they were not modelled appropriately. For example, collimators can be constructed by casting a mould or by folding plates, the former has the same septal thickness throughout whereas the latter has double the septal

Fig. 2



The model of the neuroscanner headrest.

Table 1 Collimator specifications

Collimator	Hole length (mm)	Hole size (mm)	Septal thickness (mm)
LEUHR	40	1.4	0.16

thickness in one direction compared with others – this has implications on the energy spectrum, sensitivity and the spatial resolution [8]. The LEUHR (low-energy ultra-high-resolution) collimator was modelled. Most of the required information regarding these collimators such as hole length, hole size and septal thickness (Table 1) was provided by the manufacturer. The orientation of the hexagonal columns was assumed to be in an array with the horizontal edges parallel (Fig. 3).

A 6.5-mm thick NaI(Tl) crystal was placed behind each of the collimators. As the GATE simulation detects the γ photons interacting with the crystal directly, we did not have to create a model for the light guide, the 60 PMTs and the electronics at the back of the detector head. Instead, we filled the remaining area of the detector head (between the crystal and the shielding) with a single block of glass, as used by Vieira *et al.* [16]. This approach is deemed suitable for low-energy applications as it accounts for the scatter from the back-compartment whilst providing similar results to a more detailed model [26].

Model validation

The scanner model was validated by comparing both static and SPECT imaging simulations against experimental data. The most commonly reported measurements used to validate GATE models in the literature include energy resolution, planar spatial resolution and sensitivity. In addition to the commonly reported planar imaging measures, SPECT spatial

resolution was investigated to confirm that the model produces similar SPECT images to the experimental output. A summary of the parameters used for each simulation and experimental acquisition is contained in Table 2.

Energy resolution

The energy resolution was taken from ^{99m}Tc line source acquisitions. The energy resolution full-width at half-maximum (FWHM) was calculated using Matlab (The Mathworks Inc., Natick, Massachusetts, USA) and ROOT graphing software included as part of GATE.

Planar spatial resolution

Three line sources were used experimentally to provide an average measure of the system planar spatial resolution. Three thin capillary tubes were filled with ^{99m}Tc and placed on a thin Perspex table at the centre of the scanner. The line sources were fixed at 6 cm apart with the central source in line with the centre of the detector. The capillary tubes were then rotated ninety degrees around the central tube and a second image was acquired. Each capillary tube contained ~ 10 MBq of activity and each acquisition took 600 s. The experimental set-up was recreated within GATE. Each tube was given 10 MBq of ^{99m}Tc evenly distributed within the tube. As described earlier, the acquisition time had to be reduced from 600 s to just 60 s in the simulation. The experimental images

were down-sampled following a Poisson distribution to match the simulation.

Using the software provided by Hermes, count profiles were produced perpendicular to the source orientation. These count profiles were exported to Matlab to identify the FWHM.

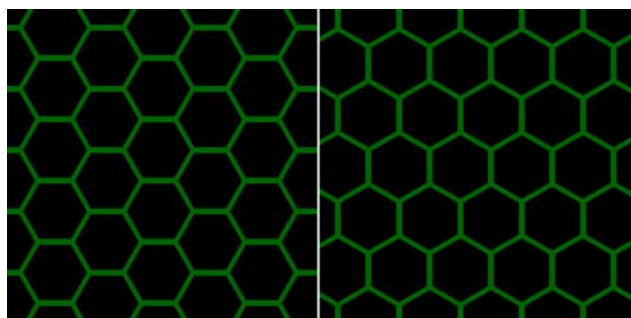
Sensitivity

The sensitivity phantom consists of a thin, hollow, square Perspex plate (GCAT, Glasgow, UK) filled with a solution of the radioisotope. The plate is attached to four thin plastic stilts and placed directly on the collimator surface. The phantom contained 20 MBq of ^{99m}Tc at the time of acquisition. A model of the sensitivity phantom was created in GATE. Similar to the spatial resolution comparison, the experimental acquisition was taken over 600 s and the simulation was taken over 60 s. The experimental images were down-sampled following a Poisson distribution to match the simulation. The sensitivity is calculated using Eq. (1):

$$\text{Sensitivity} = \frac{\text{counts}}{\text{time} \times \text{activity}}. \quad (1)$$

The experimental and simulated projection images were both analysed using the Hermes software. The number of counts obtained was found by creating a square region of interest around the phantom area. The sensitivity was tested on the two heads above and below the phantom for both the simulated and experimental data.

Fig. 3



The two potential hexagonal array orientations.

Table 2 Summary of the parameters used of each simulation and experimental acquisition

Measurements	Activity (MBq)	Acquisition time (s)	Energy window (%)	Approximate time to run simulation (days)
Planar spatial resolution				
Experimental	29	600	10	3
Simulated	30	60	10	
Sensitivity				
Experimental	20	600	10	2
Simulated	20	60	10	
SPECT spatial resolution				
Experimental	490	1920	10	8
Simulated	300	192	10	

SPECT, single-photon emission computed tomography.

SPECT spatial resolution

Comparisons of SPECT parameters such as spatial resolution are less frequently investigated when validating a GATE model. These parameters provide qualitative assessments of SPECT performance. In order to assess SPECT spatial resolution in the neuroscanner, a smaller version of the Jaszczak phantom, the mini-Jaszczak (Fig. 4), was used. The mini-Jaszczak consists of an outer Perspex cylinder containing cold spheres (with diameters 6.4, 9.5, 12.7, 15.9, 19.1, and 25.4 mm) and rods (with diameters 4.8, 6.4, 7.9, 9.5, 11.1, and 12.7 mm) and is filled with water and ~ 500 MBq of ^{99m}Tc . The SPECT acquisition included 32 projections/head (128 in total) with each head rotating 90° . Each projection was acquired over 1 min. The experimental images were down-sampled following a Poisson distribution to match the simulation.

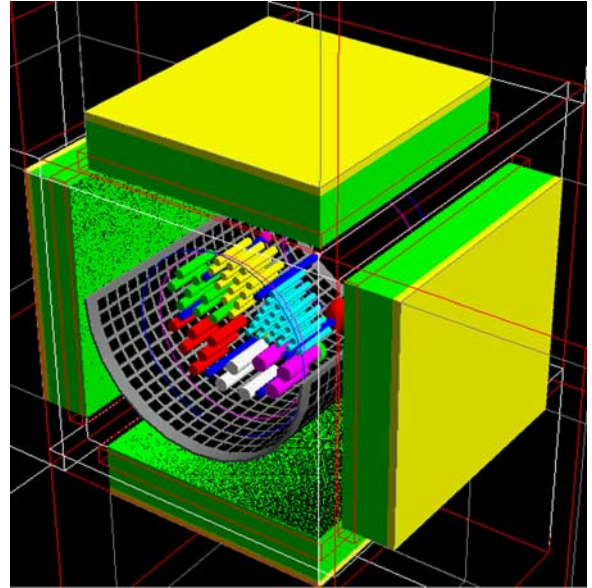
Each of the six spheres on columns and 44 rods in a 'pie' phantom arrangement were individually modelled and positioned in GATE (Fig. 5). A full model containing the mini-Jaszczak phantom resting on the headrest and surrounded by the four detector heads is shown in Fig. 6. The mini-Jaszczak simulation was run using a source activity of 300 MBq by splitting the simulation into 32 clusters (one cluster/projection). As performed in the static simulations, the simulated acquisition time was cut to one-tenth, meaning

Fig. 4



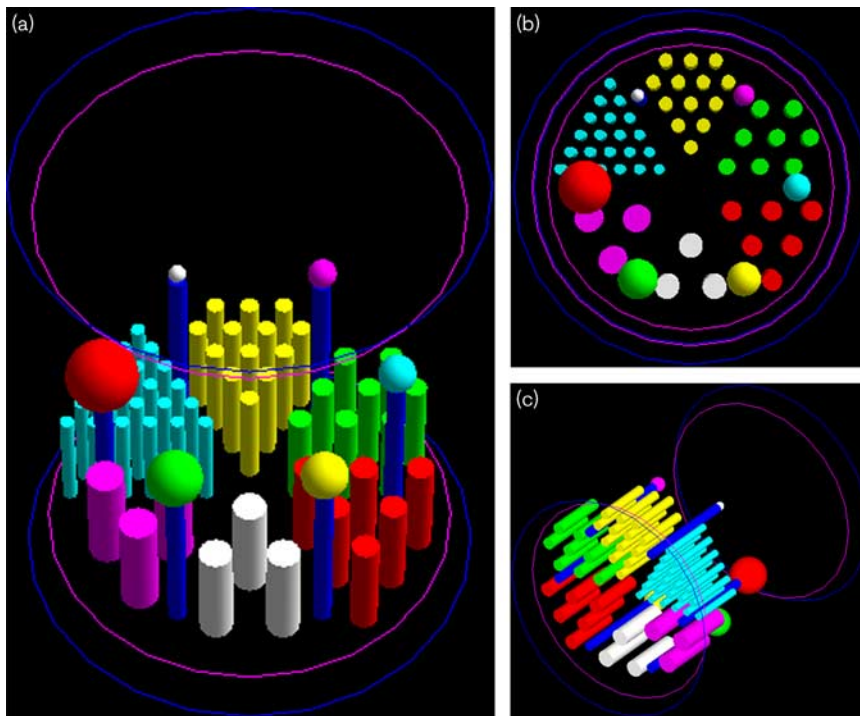
The mini-Jaszczak phantom (including both spheres and rods) Leakage of phantom shown by arrow.

Fig. 6



A full model containing the mini-Jaszczak phantom resting on the headrest and surrounded by the four detector heads.

Fig. 5



Complete GATE model of the mini-Jaszczak phantom (including both spheres and rods).

each projection took 6 s. While the activity simulated was also lower than used experimentally, it was considered as an acceptable balance between using a high activity while

minimizing the length of time the simulations took to run (still over 1 week in length). Both simulated and experimental images were reconstructed using Hermes HybridRecon

Neurology v1.1B software (Hermes Medical Solutions, Stockholm, Sweden). The approach used eight iterations and 16 subsets. Attenuation correction, resolution recovery and scatter correction were not performed.

Results

Energy resolution

The experimental FWHM was calculated to be 12.3 keV, which corresponds to an energy resolution of 8.8%. The simulated FWHM was measured to be 12 keV, giving an energy resolution of 8.6%.

The specified intrinsic energy resolution for the scanner is less than 9.7%. Both the experimental and simulated system energy resolution results were within this specified value.

Planar spatial resolution

The average simulated FWHM was found to be 5.69 (SD: 0.13) mm. The experimental line sources produced an average FWHM value of 5.64 (SD: 1.06) mm. The spatial resolutions obtained were well matched.

Sensitivity

The two camera heads accumulated 518 316 and 536 689 counts during the experimental sensitivity acquisition. When down-sampled following a Poisson distribution these reduced to 51 291 and 53 197 counts. Using an acquisition time of 60 s and 20 MBq activity, this gave a sensitivity of 42.7 and 44.3 cps/MBq.

The simulated counts were a little higher (57 321 and 65 208 counts) than expected compared to the down-sampled experimental counts but the sensitivities were fairly similar to the experimental results: 47.8 and 54.3 cps/MBq. These results are summarized in Table 3.

In the collimator datasheet provided by Mediso, the specified system sensitivity for the LEUHR collimators is 90 cpm/ μ Ci (41 cps/MBq). The higher values obtained in both the sensitivity measurements appear to be reasonable.

SPECT spatial resolution

The experimental reconstructed images are shown in Fig. 7 and the simulated reconstructed images are shown in Fig. 8.

Looking at the spheres, it seems both simulated and experimental images are able to resolve four (possibly five) of the six spheres. The edges around the spheres are much smoother in the experimental image but this is because of the larger pixel sizes. It is possible to resolve rods in several sections of the 'pie' phantom, with the simulated and experimental images appearing similar.

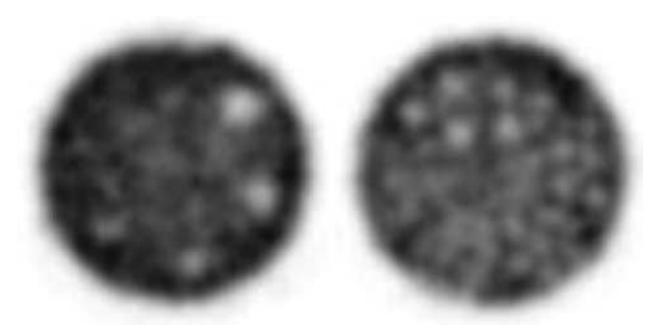
Discussion

All simulated quantitative parameters of scanner performance were broadly similar to experimental values and

Table 3 Simulated and experimental sensitivity summary

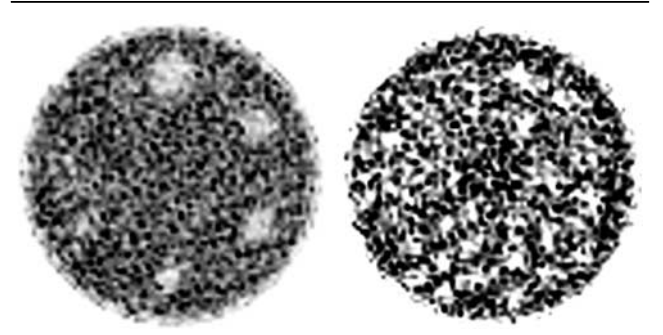
	Sensitivity (cps/MBq)
Head 1	
Simulated	47.8
Experimental	42.7
Head 3	
Simulated	54.3
Experimental	44.3

Fig. 7



Mini-Jaszczak experimental acquisition in grey scale to emphasize the spheres and 'pie' phantom. The experimental images were down-sampled following a Poisson distribution to match the simulation.

Fig. 8



Mini-Jaszczak simulated acquisition in grey scale to emphasize the spheres and 'pie' phantom.

well matched to manufacturer specifications. Both the simulated energy and planar spatial resolutions were found to show close agreement. Sensitivity measurements were less well matched, however, GATE has been known to overestimate the sensitivity values because the models often do not account for the dead spaces between PMTs [16]. The number of counts, and therefore the sensitivity, detected on head 3 was higher than head 1 because the sensitivity phantom stilts were placed on head 3 and so the source was slightly closer to it than head 1.

The simulated results generally produced slightly better results than obtained experimentally. This may be

because of some of the assumptions made by the model such as the fact that the back-compartment was not included in the model and that the collimators and crystal in the model contain fewer imperfections compared with the experimental scanner. Furthermore, the distribution and activity of the radioactive source provide additional uncertainty compared with the precise simulation set-up. However, the approach used to model the photoelectric effect, Compton and Rayleigh scattering process is not expected to be a major source of error as it is appropriate for the energy ranges used and is well validated in the literature with a strong agreement with experimental results [8].

SPECT simulations using high activity sources are rarely performed when validating a scanner model. This may be because of the high computational power required. The SPECT spatial resolution images produced from the simulation are reasonably similar to the down-sampled experimental images. These results suggest that the model has a comparable SPECT spatial resolution to the real scanner. While it would be beneficial to run the simulations with an identical activity and acquisition time to the experimental acquisitions, the work performed shows that GATE is able to simulate the neuroscanner in SPECT and well as planar simulations. Dead time effects were not modelled as it is not compatible when using ARF to acceleration the simulation. However, the gamma cameras would be expected to have a nonlinear count rate around 1–2 GBq so this was not considered a limitation.

A potential source of error in these measurements is the lower acquisition time of all simulations because of computing limitations. It is unclear to what extent this has influenced the results obtained but future work may include repeating the simulations using a large processing cluster to investigate whether the results obtained are independent of acquisition time over the acquisition timescales investigated in this study.

When attempting to optimize clinical protocols an unavoidable difficulty is in trying to decide on the ‘best’ tomographic image of an object when we do not know the specific activity distribution in that object. Phantom acquisitions, where we can acquire a known activity distribution, provide a necessary but not sufficient step in protocol optimization. This is an area where Monte Carlo simulations could be of clinical value. Take, for example, the decision to replace uniform attenuation correction methods with computed tomography (CT) attenuation correction in SPECT neuroimaging. If an a priori count distribution is known in a detailed anthropomorphic phantom, or in a set of anatomical patient scans, then we can make more informed choices about how different reconstruction parameters affect the final image. Similarly, if we can replicate detailed patient brain anatomy then we can simulate different levels of activities or

scan acquisition times and make evidence-based decisions on administered activity and acquisition parameters necessary to visualize structures of interest.

A more ambitious goal would be to utilize simulations to tailor individual scans to a particular patient. If simulation times can be sufficiently accelerated then a personalized healthcare approach based on individual patient anatomy is feasible. This is especially important for patients who deviate from the ‘standard anatomy’ used in anthropomorphic phantoms such as patients with tumours, significant atrophy, stroke patients or patients with other gross brain atrophy. By using individual patient images it is hoped that doses and acquisition times could be individually optimized on a case-by-case basis – making the process safer and more tolerable for patients and more efficient for service delivery in terms of appointment lengths. This personalized dose optimization approach would also be particularly beneficial in paediatric nuclear medicine imaging.

The future directions for work using GATE involve performing simulations with clinical level activities and realistic patient models using either anthropomorphic phantoms or actual data obtained using high-resolution imaging techniques such as CT or MRI. It is envisioned that creating simulations using these setups would guide the development and optimization of acquisition and reconstruction protocols.

Conclusion

The work undertaken during this project has laid the foundations for an approach that has the potential to improve patient care during nuclear imaging investigations by reducing patient dose and/or acquisition time. These methods have wide-ranging potential benefits as they can also be applied to other imaging systems, for example, PET and CT, to optimize new protocols on current systems or to test new equipment or prototypes. To become clinically viable, however, considerable investment is essential to provide the computational power required to perform simulations within a clinically acceptable timeframe.

Acknowledgements

The authors thank all the staff in the Nuclear Medicine departments at Glasgow Royal Infirmary and Queen Elizabeth University Hospital for their assistance throughout the project. They also thank Kiran Joshi at The Christie NHS Foundation Trust and Susan Ellam at Hermes Medical for their help in setting up the cluster computing and converting the simulation output into Hermes Interfile format respectively.

Conflicts of interest

There are no conflicts of interest.

References

- 1 Harrison RL, Haynor DR, Gillispie SB, Vannoy SD, Kaplan MS, Lewellen TK. A public-domain simulation system for emission tomography – photon

- tracking through heterogeneous attenuation using importance sampling. *J Nucl Med* 1993; **34**:P60.
- 2 Ljungberg M, Strand S-E. A Monte Carlo program for the simulation of scintillation camera characteristics. *Comput Methods Programs Biomed* 1989; **29**:257–272.
 - 3 Agostinelli S, Allison J, Amako K, Apostolakis J, Araujo H, Lucretia TK, *et al.* GEANT4 – a simulation toolkit. *Nucl Instrum Methods Phys Res A* 2003; **506**:250–303.
 - 4 Baro J, Sempau J, Fernández-Varea JM, Salvat F, *et al.* PENELOPE – an algorithm for Monte-Carlo simulation of the penetration and energy-loss of electrons and positrons in matter. *Nucl Instrum Methods Phys Res B* 1995; **100**:31–46.
 - 5 Nelson WR, Hirayama H, Rogers DW. *EGS4 code system*. Menlo Park, CA: Stanford Linear Accelerator Center; 1985.
 - 6 Briesmeister JF. *MCNPTM-A general Monte Carlo N-particle transport code Version 4C, LA-13709-M*. Los Alamos, NM: Los Alamos National Laboratory; 2000.
 - 7 Jan S, Santin G, Strul D, Staelens S, Assié K, Autret D, *et al.* GATE: a simulation toolkit for PET and SPECT. *Phys Med Biol* 2004; **49**:4543–4561.
 - 8 Staelens S, Strul D, Santin G, Vandenberghe S, Koole M, D'Asseler Y, *et al.* Monte Carlo simulations of a scintillation camera using GATE: validation and application modelling. *Phys Med Biol* 2003; **48**:3021–3042.
 - 9 Assié K, Gardin I, Véra P, Buvat I. Validation of the Monte Carlo simulator GATE for indium-111 imaging. *Phys Med Biol* 2005; **50**:3113–3125.
 - 10 Autret D, Bitar A, Ferrer L, Lisbona A, Bardiès M. Monte Carlo modeling of gamma cameras for I-131 imaging in targeted radiotherapy. *Cancer Biother Radiopharm* 2005; **20**:77–84.
 - 11 Momenzadeh M, Sadeghi R, Nasseri S. Development of GATE Monte Carlo simulation for a dual-head gamma camera. *Radiol Phys Technol* 2012; **5**:222–228.
 - 12 Imbert L, Galbrun E, Odille F, Poussier S, Noel A, Wolf D, *et al.* Assessment of a Monte-Carlo simulation of SPECT recordings from a new-generation heart-centric semiconductor camera: from point sources to human images. *Phys Med Biol* 2015; **60**:1007–1018.
 - 13 Mao Y, Yu Z, Zeng GL. Segmented slant hole collimator for stationary cardiac SPECT: Monte Carlo simulations. *Med Phys* 2015; **42**:5426–5434.
 - 14 Alzimami KS, Sassi SA, Alkhorayef MA, Spyrou NM. Preliminary Monte Carlo study of (18)F-FDG SPECT imaging with LaBr(3):Ce Crystal-based Gamma Cameras. *Conf Proc IEEE Eng Med Biol Soc* 2010; **2010**:3089–3092.
 - 15 Myronakis ME, Darambara DG. Monte Carlo investigation of charge-transport effects on energy resolution and detection efficiency of pixelated CZT detectors for SPECT/PET applications. *Med Phys* 2011; **38**:455–467.
 - 16 Vieira L, Vaz TF, Costa DC, Almeida P. Monte Carlo simulation of the basic features of the GE Millennium MG single photon emission computed tomography gamma camera. *Rev Esp Med Nucl Imagen Mol* 2014; **33**:6–13.
 - 17 Vieira L, Costa DC, Almeida P. The influence of number of counts in the myocardium in the determination of reproducible functional parameters in gated-SPECT studies simulated with GATE. *Rev Esp Med Nucl Imagen Mol* 2015; **34**:339–344.
 - 18 Hermes Medical Solutions. *SPECT reconstruction and analysis software*. Stockholm, Sweden: Hermes Medical Solutions; 2016.
 - 19 Descourt P, Carlier T, Du Y, Song X, Buvat I, Frey EC, *et al.* Implementation of angular response function modeling in SPECT simulations with GATE. *Phys Med Biol* 2010; **55**:253–266.
 - 20 De Beenhouwer J, Staelens S, Kruecker D, Ferrer L, D'Asseler Y, Lemahieu I, *et al.* Cluster computing software for GATE simulations. *Med Phys* 2007; **34**:1926–1933.
 - 21 Lazaro D, El Bitar Z, Breton V, Hill D, Buvat I. Fully 3D Monte Carlo reconstruction in SPECT: a feasibility study. *Phys Med Biol* 2005; **50**:3739–3754.
 - 22 Lee S, Gregor J, Osborne D. Development and validation of a complete GATE model of the Siemens Inveon trimodal imaging platform. *Mol Imaging* 2013; **12**:1–13.
 - 23 Rehfeld NS, Vauclin S, Stute S, Buvat I. Multidimensional B-spline parameterization of the detection probability of PET systems to improve the efficiency of Monte Carlo simulations. *Phys Med Biol* 2010; **55**:3339–3361.
 - 24 Taschereau R, Chatziioannou AF. Compressed voxels for high-resolution phantom simulations in GATE. *Mol Imaging Biol* 2008; **10**:40–47.
 - 25 Fleming JS, Kemp PM, Bolt L, Goatman KA. Measurement of cerebral perfusion volume and ^{99m}Tc-HMPAO uptake using SPECT in controls and patients with Alzheimer's disease. *Nucl Med Commun* 2002; **23**:1057–1064.
 - 26 Rault E, Staelens S, Van Holen R, De Beenhouwer J, Vandenberghe S. Accurate Monte Carlo modelling of the back compartments of SPECT cameras. *Phys Med Biol* 2011; **56**:87–104.